Astron. Astrophys. 356, 308–314 (2000)

ASTRONOMY AND ASTROPHYSICS

Dynamics of the upper solar photosphere

A. Hanslmeier[1], **A. Kučera**[2], **J. Rybák**[2], **B. Neunteufel**[1], **and H. Wöhl**[3]

[1] Institute for Geophysics, Astrophysics and Meteorology, Universitäts-Platz 5, 8010 Graz, Austria (arh@igam06ws@kfunigraz.ac.at)
[2] Astronomical Institute of the Slovak Academy of Sciences, 05960, Tatranska Lomnica, Slovakia
[3] Kiepenheuer-Institut für Sonnenphysik, Schöneckstrasse 6, 79104 Freiburg, Germany (hw@kis.uni-freiburg.de)

Received 16 June 1999 / Accepted 3 January 2000

Abstract. The dynamics of the upper solar photosphere was studied by using 1-D photospheric line spectrograms obtained using the VTT of the Observatorio del Teide. Three spectral lines with line core formation heights between 250 and 500 km were analyzed. It is clearly seen that at these levels the velocity and intensity fields are highly correlated but different from the lower lying zone where convective motions predominate. This is shown by classical methods (using correlations and bisectors) as well as by applying the Hurst exponent method to the data.

Key words: convection – Sun: atmosphere – Sun: granulation – Sun: photosphere

1. Introduction

The dynamics of the solar photosphere is characterized by two different regimes: a) below a certain height purely convectively driven motions plus oscillations and b) above a certain height by mainly non-convective, often called secondary motions and oscillations.

Kneer et al. (1980) did a coherence analysis of granular intensity by comparing the coherence between intensity fluctuations in the continuum and the wings of the line. They found a breakdown of the coherences when approaching a certain distance from the line center. Komm et al. (1990) made a power and coherence analysis of intensity variations derived from the wings of the Mg b_2 line. For the deep photosphere they found the $-5/3$ scaling law of Kolmogorov but the value of the exponent and the rms-intensity decreased with height and reaches a minimum at about 170 km. Smaller structures are coherent up to higher photospheric layers whereas the coherence for larger structures breaks down in the same layers where the rms-intensity shows a minimum. The conclusion of that paper was that large intensity structures are a result of convective overshoot and small structures are of turbulent origin. A similar result was obtained by Canfield & Mehltretter (1973). They analyzed the correlation between continuum intensity fluctuations and the vertical velocity component and found a decreasing correlation with height and a negative correlation in layers above 160 km. Nesis & Mattig (1989) showed that granular convective structures disappear up to a height of 160-200 km. In the paper of Espagnet et al. (1993) the power spectrum of velocity fluctuations was found to decrease with a $-5/3$ power law, suggesting their turbulent origin, the power spectrum of the intensity fluctuations can be fitted by two straight lines, with a $-5/3$ slope for large granules and a $-17/3$ slope for small granules. Bendlin & Volkmer (1993) studied the vertical penetration of granulation structures by scanning through the Fe I 6303Å line from near the continuum to the line center with a FPI (passband to 22mÅ). They found that even up to the line core formation height of 290 km (predicted by LTE calculations) small structures can be followed. Salucci et al. (1994) used a FPI and a UBF at Sac Peak Observatory and studied the height dependence of coherence and phase spectra. They found that most granules which reach the higher levels coherently are of larger size and only a few of them are small granules.

Salucci et al. (1994) found no correlation between the convective structures of the lower photosphere and the intensity or velocity structures of the higher photosphere in the range of $4 < k < 10 Mm^{-1}$.

So one can say that the correlations between the small-scale structures in the upper and lower photosphere is still an open question.

In Espagnet et al. (1995) a 16 min time series of two dimensional Multichannel Subtractive Double Pass spectrograms, recorded in the NaD_2 line was used to study the vertical structure of solar granulation and the penetration in the photosphere. They found that the intensity features in the upper photosphere are not related to the granules whereas the velocity fluctuations are associated to granulation over the whole photosphere.

Gadun & Pikalov (1996) used two-dimensional, non-stationary HD models of solar granulation to obtain power spectra. In sub-photospheric layers near the continuum forming level the spatial temperature spectrum corresponds to a sharper law than the spatial kinetic energy spectrum because of the influence of the radiative energy transfer and thermal conductivity on the small scale temperature inhomogeneities. As a result of increased cooling time, in the photospheric layers the ratio between the spatial temperature spectrum and the spatial kinetic energy power spectrum changes, also because of the genera-

Send offprint requests to: A. Hanslmeier

Table 1. Line characteristics of the used lines, W_λ denotes the equivalent width, h the line formation height (Kučera et al. 1995).

λ [Å]	W_λ [mÅ]	h LTE [km]	CCD camera
6301.508	127	340	ATE
6302.499	83	250	ATE
6494.994	165	500	ATC

Table 2. List of the used original spectral frames with the intensity contrast I_{rms} and the time of the exposure.

Frame	λ	λ	UT
162	6301, 6302	6494	7:44:28
163	6301, 6302	6494	7:44:36
166	6301, 6302	6494	7:45:00
167	6301, 6302	6494	7:45:05
168	6301, 6302	6494	7:45:12

tion of small scale temperature fluctuations by horizontal and vertical velocities.

Wiehr & Kneer (1988) used a highly resolved spectrogram to study the coherence between continuum intensity and line core shift. For deeply forming lines, they found well correlated shifts with continuum intensity for larger scales. For smaller scales this correlation was lost.

Many works of high resolution solar photospheric line analysis are based on deeply formed lines since mainly the convective motions were investigated (see e.g. Hanslmeier et al. 1990, 1991). In this paper only relatively high forming photospheric lines are studied by means of classical statistical tools like correlation analysis etc. Also the behavior of the line bisectors is compared with results of other studied lines. Such an analysis permits to answer the question what kind of motions in these higher layers dominates and whether these motions are temporally and spatially correlated.

2. Observations

2.1. Instruments

The spectra investigated here were taken on June 11, 1994 at the VTT telescope. A detailed description of this telescope can be found in Schröter et al. (1985). Using four 512×512 CCD cameras 3 lines were recorded. In that case 1 pixel corresponded to 3.4 mÅ in the dispersion direction and 0.17 arcsec in the spatial direction. The strictly simultaneous exposures were performed with the integration time of 0.2 sec. A more detailed description of the spectrograph setup is given by Kučera et al. (1995).

The characteristics of the observed FeI lines are given in Table 1.

2.2. Data reduction

The data were treated in the traditional way i.e the dark currents were subtracted and they were flat field corrected. The flat field was taken by moving the telescope over the solar disk. Unfortunately after applying these procedures still some sawtooth like features remained. These features appear due to small shifts between the flat field matrix and the spectrum caused by the temporal motion or tilt of the spectrograph mechanical parts. In fact two influences appear in the flat field matrix: a) the effects coming only from the slit (defects on the edges of the slit, dust on the slit etc.) and b) the defects of the chip and of the camera window (wrong pixels, dust on the window etc.). The first part could be denoted *slit flat field* and the second part *camera flat field*. The second part is stable in time. We separated the two parts of the flat field matrix and shifted only the slit flat fields to fit the spectrum position. Then the slit and camera flat fields were added together and applied to correct the spectrum. In order to correct the spectra for this first the spectral lines had to be aligned perpendicular to the upper border of the chip.

After applying all these procedures the data were selected according to the following quality criteria: a) we calculated the rms intensity fluctuations I_{rms} in the continuum nearby the lines and b) we calculated the power spectra and determined where the power reaches noise level. It was found that for the best spectra, the I_{rms} was about 0.046 and the noise level was reached at about 0.42 arcsec. Thus from the whole time series, a set of spectra listed in Table 2 was selected. They were taken in the same position near the disk center (μ = 0.99). For these spectra the following spectral line characteristics along the slit length of 85 arc seconds (512 pixels) were calculated: I_c – the continuum intensity, I_r – the residual line center intensity, v_r – the line center Doppler velocity, $fwhm$ – the full width at half minimum and the bisectors of the line profiles including v_c – the Doppler shift velocity near the top part of the line bisector.

We also tried to eliminate the influence of oscillatory motions by applying a spatial filtering procedure that is described e.g. in Mattig & Schlebbe (1974). After transforming the data into the Fourier domain at a frequency of $k_0 = 2.3Mm^{-1} = 3.''6$ a cutoff mask is convolved thus separating small scale convective motions from larger scale mainly oscillatory motions. Since no time series are available a proper separation between these two types of motion in the $k - \omega$ space was not possible.

3. Results

3.1. Correlations

We calculated the correlations between different line parameters. Especially the correlations between line center velocities v_r and line center residual intensities I_r were studied. In Fig. 1 the correlations between different line center velocities are given as a function of Δh which denotes the difference in line core formation height. These correlations have been calculated for all 5 different sets of spectra that means we can see a very small time evolution of these correlations since spectrum 162 was taken about 1 min earlier than spectrum 168. Although the time separation between these spectrograms is very small the individual examples can be used in order to demonstrate the statistical significance of the results. In all cases the correlation

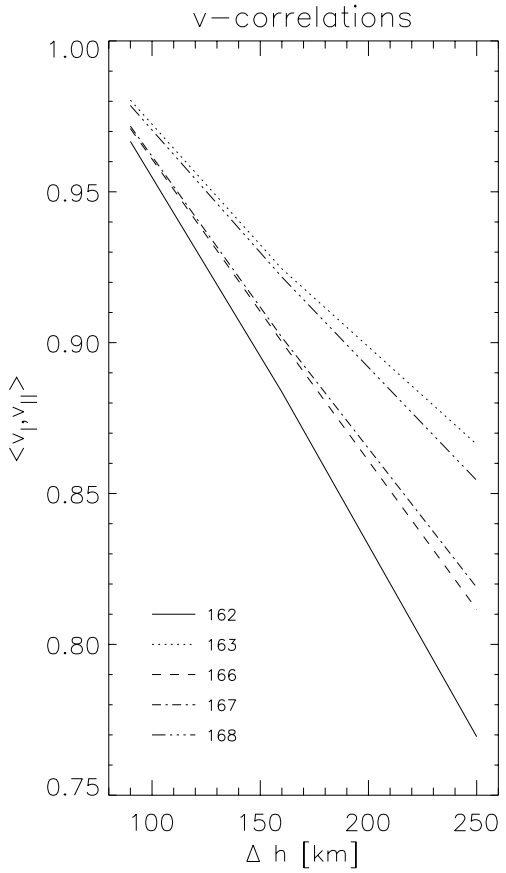

Fig. 1. Correlations between the line center velocities v_r. The difference in formation height between the different lines is denoted by Δh. The numbers 162, 163, 166, 167, 168 stem for the different frames.

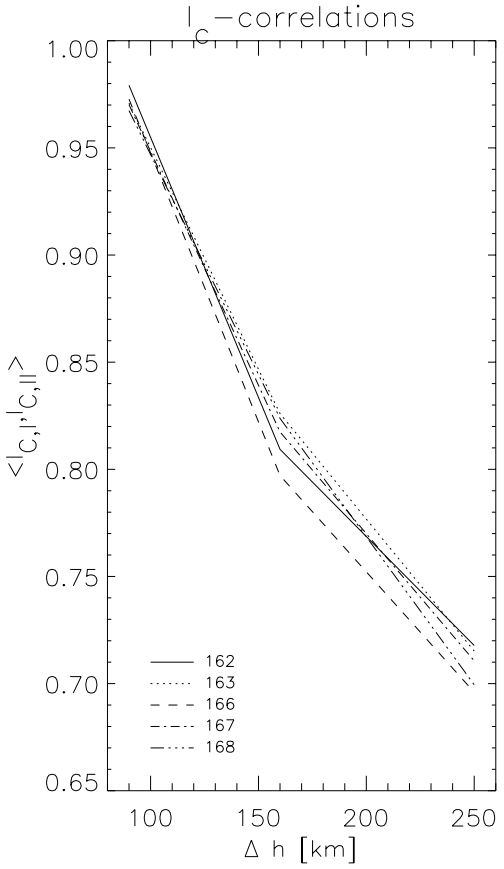

Fig. 2. Correlations between line center residual intensities I_r. Δh denotes the difference in formation height between the different lines. The numbers 162, 163, 166, 167, 168 denote the different set of frames.

linearly decrease with increasing Δh. Please note that even at a large height difference of about 250 km there is still a reasonable correlation between the line center velocities of about 0.76. The same correlations were also analysed for the filtered data, but the differences were quite small so the figures are not given here.

In Fig. 2 the correlations between the line center residual intensities I_r are given in the same way as in Fig. 1 as a function of Δh and for the different spectra used. Again one can see very high correlations between the residual intensities for low Δh values, and these correlations fall down very steeply. At a $\Delta h \sim 150$ km however in all 5 cases the gradient becomes less steep and at a $\Delta h \sim 250$ km we still have a correlation of about 0.70.

We also studied the correlations between other line parameters such as full width at half maximum, equivalent width and the above mentioned parameters.

The correlations between continuum intensity I_c and line center velocity v_r with these parameters were relatively low, there was no unique trend and the dispersion between the different spectra analyzed was relatively high. Only in the case of correlations between line center residual intensities I_r and these line parameters, the values were in some cases above 0.50 indicating some correlation. The results are given in Table 3.

The correlation values for the filtered data are given in brackets. They only slightly differ from the values for the unfiltered data.

Table 3. The correlation coefficients of the line center residual intensity I_r and other spectral line parameters.

λ	Frame	$\langle I_r, v_r \rangle$	$\langle I_r, W_\lambda \rangle$	$\langle I_r, fhwm \rangle$
6302	162	0.45 (0.45)	-0.68 (-0.73)	0.54 (0.53)
6302	163	0.47 (0.33)	-0.74 (-0.69)	0.67 (0.61)
6302	166	0.28 (0.40)	-0.41 (-0.26)	0.57 (0.55)
6302	167	0.18 (0.36)	-0.38 (0.24)	0.59 (0.51)
6302	168	0.26 (0.28)	-0.71 (-0.66)	0.59 (0.58)
6301	162	0.42 (0.40)	-0.63 (-0.63)	0.56 (0.48)
6301	163	0.47 (0.26)	-0.60 (-0.60)	0.73 (0.50)
6301	166	0.20 (0.35)	-0.36 (-0.26)	0.61 (0.44)
6301	167	0.11 (0.31)	-0.27 (0.23)	0.66 (0.38)
6301	168	0.18 (0.26)	-0.58 (-0.57)	0.68 (0.41)
6494	162	0.25 (-0.23)	-0.72 (-0.69)	0.53 (0.42)
6494	163	0.34 (-0.13)	-0.38 (0.23)	0.65 (0.41)
6494	166	-0.03 (-0.13)	-0.51 (-0.22)	0.56 (0.35)
6494	167	-0.10 (-0.09)	-0.36 (0.29)	0.64 (0.36)
6494	168	-0.04 (-0.01)	-0.44 (0.25)	0.62 (0.26)

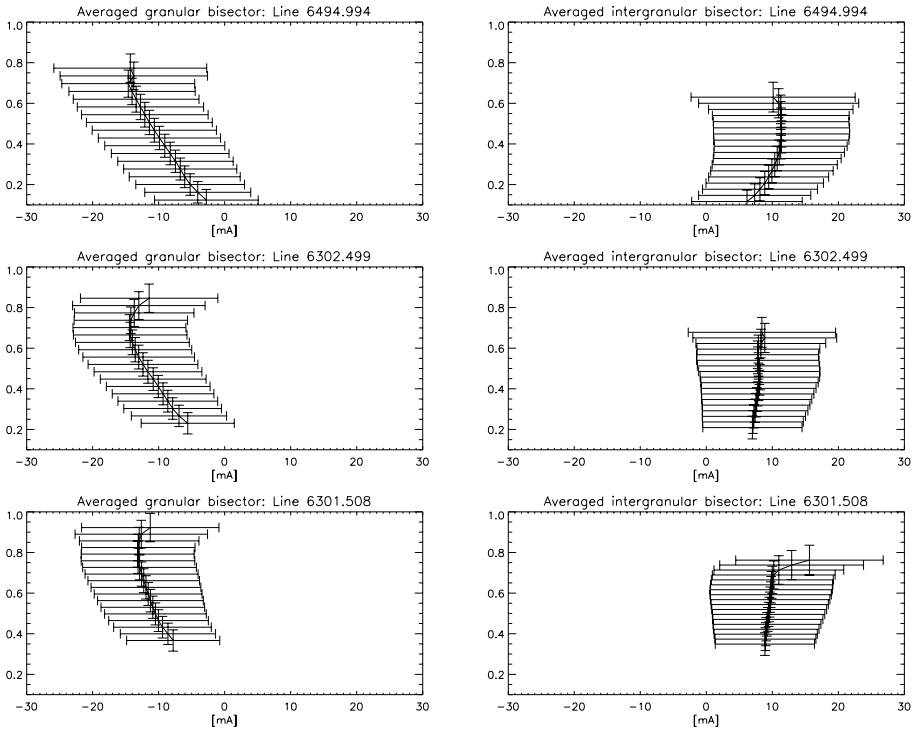

Fig. 3. Averaged granular and intergranular bisectors for spectrum nr. 162. In the case of the largest line core formation height the largest asymmetries result.

For the filtered data the differences were quite small and the results quite similar to the values given above, so these data are not given explicitly here.

3.2. Bisectors

In this section we discuss averaged bisectors. The averaging was done according to the following criterion: all continuum intensities were averaged and then we calculated "granular" bisectors belonging to continuum intensities $I_c > 1.0$ and intergranular bisectors resulting from line profiles with $I_c < 1.0$. An example of these averaged bisectors for spectrum 162 for all three line studied is given in Fig. 3.

By vertical and horizontal bars the standard deviations resulting from the averaging are indicated. One can see that these deviations are smaller near line core formation height and larger near continuum forming level.

For comparison the same procedure was repeated with the filtered data and the results can be seen in Fig. 4. It can be seen from Fig. 3 and Fig. 4 that the granular and intergranular bisectors behave differently:

- granular bisectors: the unfiltered and filtered bisectors look very similar, and appear nearly at the same position. For the filtered bisectors, the standard deviations are larger near continuum level whereas for the unfiltered bisectors the standard deviations are nearly the same at alle levels.
- intergranular bisectors: the filtered averaged bisector is clearly changed in position towards the blue and its asymmetry is reduced. Also the standard deviations are reduced quite remarkably.

Thus the filtering greatly influences on the intergranular bisector.

3.3. Hurst exponent, turbulent behavior

In Fig. 5 we give the results for the Hurst analysis (Hurst et al. 1965) which enables to distinguish the behavior of a data set between random walk, persistency and antipersistency. It is seen that all values are around 0.5. In the case of fluctuations of intensity and velocity near continuum level, the values are below 0.5 whereas for the fluctuations at line core formation height level the Hurst exponents lie above 0.5. The variation of the Hurst exponent for 3 different spectra is shown by different types of lines. The dashed-pointed line denotes the results for the filtered data. It is clearly seen that all these values are well below the 0.5 threshold and the difference between the individual spectra was insignificant.

As in many works one can define the influence of turbulent motions on the line parameter full width of half maximum ($fwhm$) in such a way, that enhanced $fwhm$ indicates turbulent motions. The question where these motions occur is treated here by investigating the correlation between the following quantities: if both $fwhm$ values as well as line center velocities v_r were positive (which means enhanced values over the average and in the case of line center velocities a redshift, thus downward motions) then a new dataset was generated consisting of values=1. Otherwise the new dataset was filled by zero values. This new data matrix was then correlated with the continuum intensity values (I_c). This correlation was designated by $\langle (v_r, fwhm), I_c \rangle$. Analogous to this correlation we calculated $\langle (v_c, fwhm), I_c \rangle$, where v_c means velocity taken from

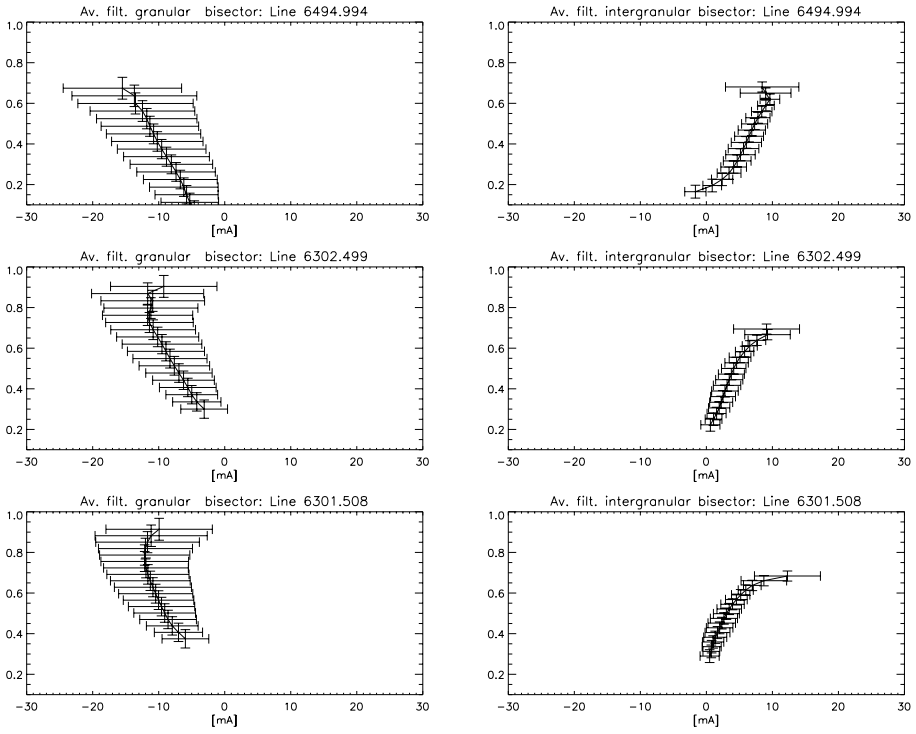

Fig. 4. Averaged filtered granular and filtered intergranular bisectors for spectrum nr. 162. In the case of the largest line core formation height the largest asymmetries result.

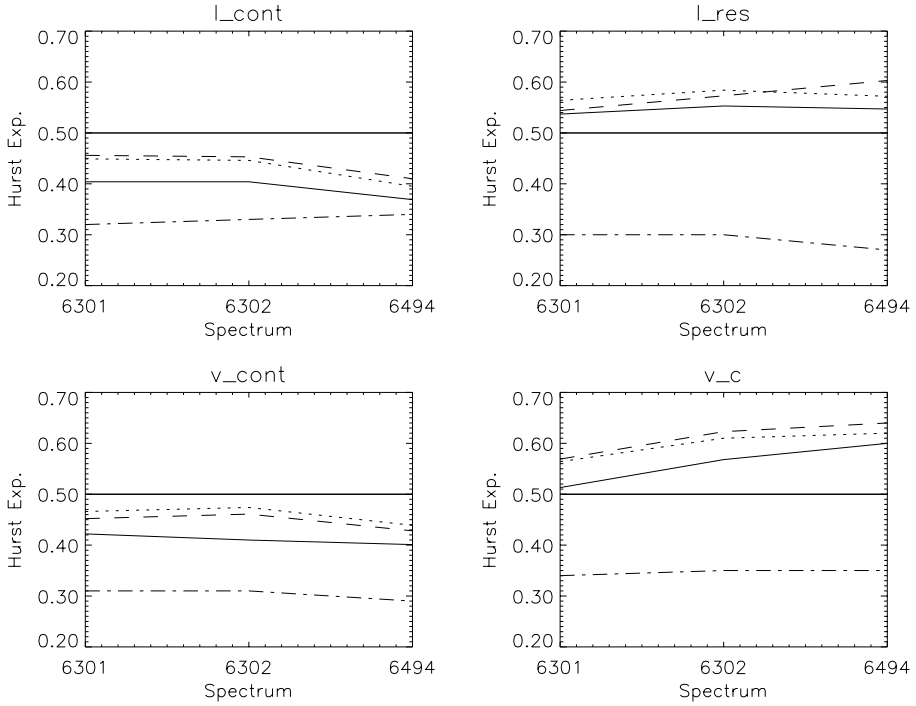

Fig. 5. Variation of the Hurst exponent of 3 investigated lines for the continuum intensity fluctuations I_c, the line center intensity fluctuations I_r, the line center velocity fluctuations v_r and the velocity fluctuations deduced from bisectors at near continuum intensity level v_c. The values for the filtered data are given in brackets.
The variation of the Hurst exponent for 3 different spectra is shown by different types of lines. The exponent value of 0.5 representing the random walk uncorrelated relation. The lowest line denotes the behavior of the filtered data.

the bisector near continuum level (which was defined here as 0.9 line depth). The result of these correlations is shown in Table 4. The correlations are very small and negligible in the case of $\langle (v_r, fwhm), I_c \rangle$ however they reach values up to 0.3 for $\langle (v_c, fwhm), I_c \rangle$. The Hurst exponent calculated for this new data matrix was around 0.20 indicating antipersistent behavior. The values for the filtered data are given in brackets and do not differ largely.

4. Discussion

Using solar photospheric lines originating in the middle up to the high photospheric level we investigated the dynamics in these layers. The correlation analysis clearly showed that both velocity fields as well as intensity fields resulting from the line core residual intensities are very well correlated for small height differences and that these correlations linearly decrease with increasing Δh. It is interesting to note that in the case of line

Table 4. Correlation coefficients of the line parameters - $\langle(v_r, fwhm), I_c\rangle$ and $\langle(v_c, fwhm), I_c\rangle$

λ	$\langle(v_r, fwhm), I_c\rangle$	$\langle(v_{cont}, fwhm), I_c\rangle$
6302	-0.24 (0.23)	-0.32 (-0.40)
6301	-0.19 (0.24)	-0.30 (-0.30)
6494	+0.06 (0.10)	-0.21 (-0.22)

core residual intensities the gradient becomes less steep when $\Delta h > 150\ km$. So we have to expect correlated temperature and velocity fields at these layers which are, on the other hand not correlated with the corresponding fields in the lower layers. This follows from the fact that we found no correlations between these parameters and the continuum intensity fluctuations. These results are in agreement with the results found by Komm et al. (1990) where it is shown that for the lower photosphere an energy cascade from large structure towards smaller ones occurs and that especially the smaller structures can penetrate into the mid photosphere. However, at a level of about 170 km above $\tau_{5000} = 1$ a transition to non-convective secondary motions occurs. The results of our paper show that these motions are remarkably well correlated. This is in agreement with the noise theory (Voss 1988) cited in the paper of Komm et al. (1990).

In this case noise means a stochastic signal and different types of noise are represented by different scaling laws of their spectral intensities $S(f)$ given by the relation:

$$S(f) \sim f^{-q} \tag{1}$$

(f denotes the frequency). White noise is random and is described by $q = 0$, the noise of electronic components is represented by $q = 1$ and for Brownian motion $q = 2$. In our case we used the following definition of this parameter: whenever in a time series there is a Brownian motion (sometimes called a random walk), the value of a quantity x (that describes the time series) on the average moves away from its initial position by an amount proportional to the square root of time. Then we may say that the Hurst exponent is 0.5. In the theory of fractional Brownian motion exponents > 0.5 indicate persistence (meaning that past trends persist into the future), whereas exponents < 0.5 indicate antipersistence (past trends reverse in the future). An exponent close to 0.5 means random uncorrelated motions. From Fig. 5 it follows that there is a clear reversal of trends when calculating the Hurst exponent for parameters calculated near the continuum and parameters calculated at the line core formation height. Discussing the correlations between $\langle(v_r, fwhm), I_c\rangle$ one can see very low values (cf. Table 4). For the correlations $\langle(v_c, fwhm), I_c\rangle$ the values are negative and around 0.3. This is still quite low. However it gives an indication that under the assumption that full width at half maximum fluctuations can be interpreted by turbulent motions. These motions occur at downflowing regions in the low photosphere. Similar correlations were calculated for the case of upflowing regions and the values found were in all case below 0.1. These facts can be interpreted by a predominance of turbulent motions near to downflow regions in the intergranulum. This has been found also in the paper of Nesis et al. (1999) using lines from the lower photosphere. In our case, since we have lines that originate higher in the photosphere, the correlations are low at the respective line core formation heights. Applying the same type of correlations instead of velocities to velocity gradients (where these gradients are taken from the variation of rms velocities along the spectrograph slit that means along a spatial coordinate on the sun) we found in all cases low correlations (below 0.2) with the $fwhm$.

The correlations between continuum intensities and line center velocities or line center intensities are very low because the lines originate at relatively high levels but considering the correlations between these parameters for lines above 200 km we find relatively large values.

Rimmele et al. (1995) and Espagnet et al. (1996) have shown that small scale oscillations (2-3 arcsec) are excited in the intergranular regions. In our data set these oscillations cannot be removed completely since we cannot apply an appropriate spatio-temporal filtering. This can also explain why the coherence between features observed at various heights is not improved in the filterd data contrary to the findings of Deubner (1988) or Espagnet et al. (1995).

The clear difference between granular and intergranular bisectors for filtered and unfiltered data shows that the filtering mainly influences intergranular bisectors. The larger standard deviations near continuum level in Fig. 4 for the filtered granular bisectors indicate that at these low levels the smaller scale convective motions dominate. The correlations are only slightly affected by the filtering process.

The bisector is found to have a different behavior in filtered and non-filtered data, but only for bisectors originating from intergranular spaces. This may be explained by the fact that the small scale oscillations, which are excited in intergranular spaces (and not by granules) are at least partly removed by our filtering process.

Acknowledgements. A.H. thanks the 'Austrian Fonds zur Förderung der wissenschaftlichen Forschung' for supporting these investigations. A.K. and J.R. acknowledge the grant 2/7229/20 and the Austrain and Slovakian Acadmey of Sciences.

References

Bendlin C., Volkmer R., 1993, A&A 278, 601
Canfield R.C., Mehltretter J.P., 1973, Sol. Phys. 33, 33
Deubner F.L., 1988, A&A 204, 301
Espagnet O., Muller R., Roudier Th., Mein N., 1993, A&A 271, 589
Espagnet O., Muller R., Roudier Th., Mein P., Mein N., 1995, A&AS 109, 79
Espagnet O., Muller R., Roudier T, Mein P., Mein N., Malherber J.M., 1996, A&A 313, 297
Gadun A.S., Pikalov K.N., 1996, Sol. Phys. 166, 43
Hanslmeier A., Mattig W., Nesis A., 1990, A&A 238, 354
Hanslmeier A., Nesis A., Mattig W., 1991, A&A 251, 307
Hurst H.E., Black R.P., Simaika Y.M., 1965, Long-Term Storage, An Experimental Study, Constable, London.
Kneer F.J., Mattig W., Nesis A., Werner W., 1980, Sol. Phys. 68, 31

Komm R., Mattig W., Nesis A., 1990, A&A 239, 340
Kučera A., Rybák J., Wöhl H., 1995, A&A 298, 917
Mattig W., Schlebbe H., 1974, Sol. Phys. 34, 299
Nesis A., Hammer R., Kiefer M., et al., 1999, A&A 345, 265
Nesis A., Mattig W., 1989, A&A 201, 153
Rimmele Th., Goode P., Harold E., Stebbins R., 1995, ApJ 444, L119-L122
Salucci G., Bertello L., Cavallini F., Ceppatelli G., Righini A., 1994, A&A, 285, 322
Schröter E.H., Soltau D., Wiehr E., 1985, Vistas Astron. 28, 519
Voss R.F., 1988, In: Peitgen H.O., Saupe D. (eds.) The Science of Fractal Images, Springer, Berlin, Heidelberg, New York.
Wiehr E., Kneer F.J., 1988, A&A 195, 310